AIP | Review of Scientific Instruments

Online tangential soft xray/VUV tomography on COMPASSC

R. D. Durst

Citation: Rev. Sci. Instrum. **61**, 2750 (1990); doi: 10.1063/1.1141969
View online: http://dx.doi.org/10.1063/1.1141969
View Table of Contents: http://rsi.aip.org/resource/1/RSINAK/v61/i10
Published by the American Institute of Physics.

Related Articles

Low-frequency linear-mode regimes in the tokamak scrape-off layer
Phys. Plasmas 19, 112103 (2012)

Spherical torus equilibria reconstructed by a two-fluid, low-collisionality model
Phys. Plasmas 19, 102512 (2012)

Oblique electron-cyclotron-emission radial and phase detector of rotating magnetic islands applied to alignment and modulation of electron-cyclotron-current-drive for neoclassical tearing mode stabilization
Rev. Sci. Instrum. 83, 103507 (2012)

Toroidal rotation of multiple species of ions in tokamak plasma driven by lower-hybrid-waves
Phys. Plasmas 19, 102505 (2012)

Perpendicular dynamics of runaway electrons in tokamak plasmas
Phys. Plasmas 19, 102504 (2012)

Additional information on Rev. Sci. Instrum.

Journal Homepage: http://rsi.aip.org
Journal Information: http://rsi.aip.org/about/about_the_journal
Top downloads: http://rsi.aip.org/features/most_downloaded
Information for Authors: http://rsi.aip.org/authors

ADVERTISEMENT

Downloaded 08 Nov 2012 to 194.81.223.66. Redistribution subject to AIP license or copyright; see http://rsi.aip.org/about/rights_and_permissions

On-line tangential soft x-ray/VUV tomography on COMPASS-C

R. D. Durst, The COMPASS Group
AEA Fusion/Euratom Association, Culham Laboratory, Abingdon OX14 3DB, England

(Presented on 7 May 1990)

A tangentially viewing pinhole camera has been used to image the COMPASS-C plasma in the vacuum ultraviolet and soft x-ray spectral regions with framing rates up to 330 Hz. The PC-based system acquires up to 256 128×128 pixel images per shot and incorporates an array processor to allow on-line tomographic reconstructions. Data compression is used to reduce the data load by a factor of 4.

I. INTRODUCTION

The COMPASS Tangential Soft X-Ray/VUV Camera (TAN SOX) uses a tangential view of the plasma to tomographically reconstruct the plasma emissivity contours[1] as previously demonstrated on CLEO[2] and PBX.[3] The soft x-ray (SXR) emissivity and vacuum ultraviolet (VUV) continuum emissivity are associated, respectively, with isotemperature and isodensity contours. In a shaped plasma this information can be used to derive the current density distribution.[4] The TAN SOX is also sensitive to nonthermal x-ray emission and has been used to diagnose the spatial distribution of suprathermal electrons in a slideaway discharge.[5]

The system has been optimized to allow fast (<15 s) tomographic reconstructions of the emissivity distribution. This allows inversions to be performed on-line to provide timely information to the machine operators and experimenters and also makes off-line data analysis more efficient and productive.

II. DESCRIPTION OF DIAGNOSTIC

The design of the pinhole camera subsystem is based on work done on PBX.[3] A 0.4 mm pinhole images the plasma onto a P-11 (ZnS:Ag) scintillator screen. This phosphor has a high quantum yield in the VUX/SXR region ($\eta = 65$ at 8.3 Å,[6] 45 times the yield of the sodium salicylate) and a fast decay time (20 μs decay to 10% of initial brightness). For a thin screen of P-11 (~ 10 mg cm^{-2}), η peaks at 3–5 keV and falls slowly with increasing incident photon energy to about 25% of the peak value at 15 keV. There is no sharp cutoff in the yield and the screen continues to respond (with reduced efficiency) to incident photons with energies up to several MeV.[7] The extended response makes the system quite sensitive to x-ray radiation from suprathermal electrons. Between the pinhole and screen is a filter wheel with three foil filters (25 μm Be, 8 μm Al, and 100 nm Al) and a VUV interference filter (140 nm, 10 nm FWHM).

The phosphor screen is fiber optically coupled to a microchannel plate (MCP) intensified photodiode camera whose photocathode response (S20) closely matches the output spectrum of the P-11 screen. The MCP gain is externally controllable from 10^3–10^6. The MCP can be gated for fast exposures (down to 5 ns).

Fast phenomena may be resolved by appropriate gating. For example, a system which gates the MCP on for a fixed portion of each sawtooth cycle during a frame has been implemented. In addition, pinhole images may be used as templates to improve reconstructions based on SXR diode array data.[8]

The camera is a Reticon MC9128 with a pixel resolution of 128×128 and a maximum framing rate of 330 Hz. The camera control and data acquisition are managed by an IBM AT compatible PC which is linked to the camera via fiber optics (see Fig. 1). An add-in board containing an Intel 8253 programmable timer provides the camera with frame timing pulses (synchronized to the plasma t_0) and the MCP gate commands. This board also provides digital output channels which are used to control the MCP gain.

Video is sent to the PC via a 50 MHz analog optical link and is digitized by a frame grabber board (Data Translation 2861). This board supports acquisition of the nonstandard video format (slow scan) produced by the MC9128 (though the driving software required modification in order to operate at framing rates greater than 60 Hz). The DT2861 has sufficient on-board memory to acquire up to 256 frames per shot and is coupled to a fast (8 MFLOPS) array processor (DT7020) which is used to tomographically invert some of the raw data between shots.

In order to maximize data availability the TAN SOX has been integrated into the COMPASS archive system. Because of the very large amounts of data that this diagnostic can generate (up to 4 MBytes per shot, though the typical data load is presently <1 MBytes) differential run length data compression[9] is performed before the data is archived. This is an information-conserving technique which exploits the high spatial correlation in the images. Consider the line of pixels through the center of the image. Typically the pixel values increase smoothly from near zero at the edge of the image to about 255 near the center (pixel 64) and the average differential between adjacent pixels is 4. Thus, while the pixel values require 8 bits for storage, the differentials can be stored using only 3 bits with no loss of information content. In practice the line is divided into a number of "runs" which correspond to areas of the image with more or less spatial structure which therefore require more or fewer bits for storage. The compression ratio achieved by this technique clearly depends on the spatial structure of a given image. Typically, com-

 0034-6748/90/102750-03$02.00 © 1990 American Institute of Physics

Downloaded 08 Nov 2012 to 194.81.223.66. Redistribution subject to AIP license or copyright; see http://rsi.aip.org/about/rights_and_permissions

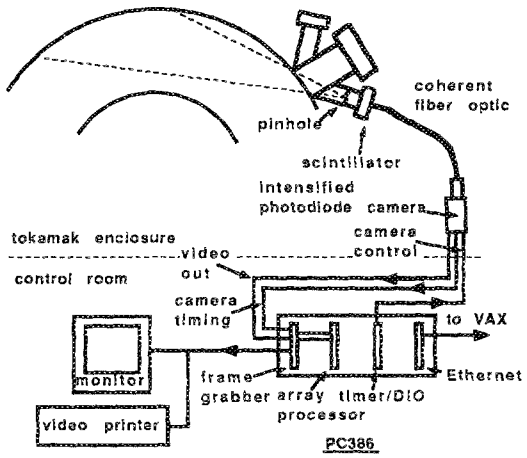

FIG. 1. Schematic diagram of the TAN SOX.

pression ratios of about 4 are achieved on TAN SOX data. The compression requires 30 s/MByte using the PC processor.

Compressed data are sent to the data archive on the main COMPASS VAX via Ethernet. The PC-VAX link is controlled by Digital's PCSA software which allows the PC to directly access VMS files. PCSA is run from extended memory using a Quarterdeck memory manager since when run in conventional memory PCSA uses nearly half the 640 kB memory available for the acquisition and analysis software.

A subset of the images can be tomographically inverted on-line by the PC between shots. The techniques used for the tomographic reconstructions are maximum entropy (ME)[10] and Bayesian regularized least squares optimization (BRLSO).[11] The reconstructions produced by these techniques are quite similar though the latter technique is more suited to on-line inversions due to its faster convergence and the ease with which it can be implemented on the fast array processor. BRLSO is one of a class of algorithms known as row action methods or algebraic reconstruction techniques (ARTs).[7] It iteratively minimizes the cost function

$$r\|b-Le\|^2+\|e^E-e\|^2, \tag{1}$$

where b is the vector of measured brightnesses, e is the solution vector (emissivity), L is the digitization matrix which is a function only of the system geometry, $\|\ \ \|^2$ represents the Euclidean norm, and e^E is the "expected solution" which, in the absence of other information can be taken a constant vector. However, where significant *a priori* information is available the use of a nontrivial e^E can greatly improve the quality of the reconstructed image as well as increase the speed of convergence. The parameter r determines the relative importance of *a priori* and measured data and is proportional to the signal-to-noise ratio. During each iteration a single brightness measurement b_{i_k} is used to adjust those emissivity elements in e which contribute to it

$$e^{k+1}=e^k+rc^kL_{i_k}, \tag{2}$$

$$u^{k+1}=u^k+c^kt_{i_k}, \tag{3}$$

where k represents the kth iteration, t_i is the vector whose ith component is one and all others are zero and c is given by

$$c^k=\lambda^k\frac{r[b_{i_k}-\langle L_{i_k},e^k\rangle]-u^k_{i_k}}{1+r^2\|L_{i_k}\|^2}, \tag{4}$$

where i_k represents the index of the brightness vector element which is used to update e, λ is a relaxation parameter such that $0<\lambda<2$ and angular brackets represent the inner vector product. Note that the simplicity of the iteration step is well suited to implementation on an array processor.

The vectors e and u are initialized to $e^0=e^E$ and $u^0=0$. As noted above, the choice of e^E is important both to the quality of the final image and the speed of convergence: a reasonable estimate of e^E can save many thousands of iterations. The following procedure is currently used to derive e^E. First, note that for any toroidally symmetric plasma the reconstruction of the emissivity in the horizontal midplane, e_H, reduces to the Abel problem. Thus, e_H can be quickly found using one of the well known techniques for Abel inversion. In particular, a generalized cross validation (GCV) smoothing spline[12] is fitted to the horizontal brightness vector and is then analytically inverted. The GCV algorithm also gives an estimate of the experimental scatter in the data which is needed to determine the regularization parameter r as well as the stopping criterion for both the BRLSO and ME algorithms.[10] A model for the overall emissivity is then fitted to e_H. A four-parameter model has been found to be suitable for making the initial estimate in circular COMPASS discharges. The geometry of the plasma is assumed to be approximated by shifted circles where the shift of any flux surface, $r_c(\rho)$, is given by

$$r_c(\rho)=r_0(1-\rho^2)+r_a, \tag{5}$$

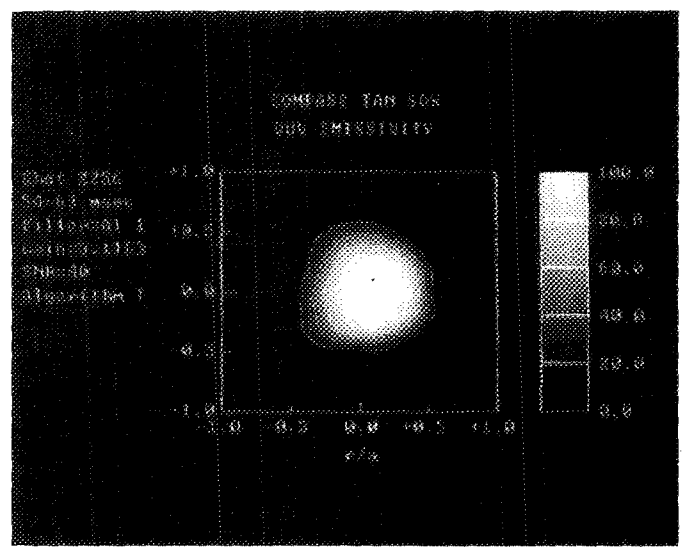

FIG. 2. Emissivity contours for a typical ohmic discharge. A 100-nm Al filter was used which transmits above 10 eV (except for a notch around 100 eV).

Downloaded 08 Nov 2012 to 194.81.223.66. Redistribution subject to AIP license or copyright; see http://rsi.aip.org/about/rights_and_permissions

where r_a is the shift of the outermost flux surface which is estimated from the edges of e_H, r_0 is the shift of the magnetic axis relative to r_a which is determined from the peak of e_H and ρ is the radial flux surface coordinate.

With the conversion from Cartesian to flux surface coordinates fixed by Eq. (5), e_H is fitted to the form

$$e_H \propto \exp(-a\rho^b), \tag{6}$$

which is then used to evaluate e^E off the midplane through the assumption that emissivity is constant on a flux surface. This fit is performed by the PC while the iterative inversion [Eqs. (2),(3)] is done by the attached array processor. Typical convergence times are 10–15 s for a 32×32 pixel inverted image. Thus, several frames can be inverted between shots.

III. TYPICAL RESULTS

Figure 2 shows the broadband VUV emissivity distribution for a typical COMPASS ohmic discharge. The discharge parameters were 80 kA, 1.4 T, and 1.1×10^{19} m^{-3}. A 100 nm Al filter was used and the integration time was 8 ms.

Figure 3 shows the SXR emissivity for an ohmic, inboard x-point discharge (90 kA, 1.1 T, 1.4×10^{19} m^{-3}). Figure 3(a) shows the basically circular plasma before the shaping fields were applied while 3(b) shows the distribution after the x point was established. Note that the SXR images are typically more peaked than those taken in the VUV (e.g., Fig. 2). Magnetic measurements indicate that the x point was near the inboard limiter midplane ($r/a=-1$, $z/a=0$ in Fig. 3) and the reconstruction in 3(b) shows a clear distortion of the originally circular distribution on the side facing the x point. Details of COMPASS inboard x-point work will be reported elsewhere.[5]

In summary, the diagnostic has been operated routinely on COMPASS-C and has produced high quality reconstructions of SXR and VUV emissivity distributions.

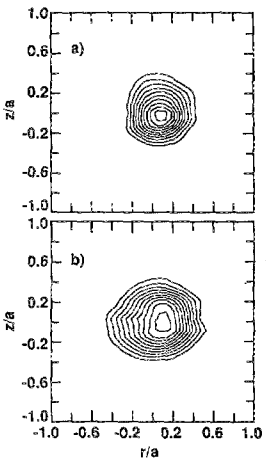

FIG. 3. SXR emissivity for an ohmic discharge with an inboard x point (shot 1871). a) shows the discharge before the shaping fields were energized (24–36 ms) while b) shows the plasma after the x point was established (60–72 ms). The 25 μm beryllium filter (2 keV) was used. The contour levels are multiples of 10%.

The key features of the system including data compression algorithms, integration with the VAX cluster (using PCSA), and the use of a fast array processor have been demonstrated.

[1] J. Schivell, IEEE Trans. Plasma Sci. **PS-8**, 226 (1980).
[2] S. Takamura, T. N. Todd, T. Edlington, and CLEO Group, Plasma Phys. Cont. Fusion **28**, 1717 (1986).
[3] R. Fonck, K. P. Jaehnig, E. T. Powell, M. Reusch, P. Roney, and M. P. Simon, Rev. Sci. Instrum. **59**, 1831 (1988).
[4] J. P. Christiansen and J. B. Taylor, Nucl. Fusion **22**, 111 (1982).
[5] R. D. Durst, P. G. Carolan, B. Parham, the COMPASS Group, Proceedings of the 17th EPS Conference, Amsterdam (1990).
[6] V. G. Movshev, N. K. Sukhodrev, and V. A. Shurygin, Opt. Spectrosc. **38**, 58 (1975).
[7] G. J. Berzins, A. H. Lumpkin, and H. L. Smith, Opt. Eng. **22**, 633 (1983).
[8] A. Holland, R. J. Fonck, E. T. Powell, and S. Sesnic, Rev. Sci. Instrum. **59**, 1819 (1988).
[9] W. K. Pratt, *Digital Image Processing* (Wiley, New York, 1978).
[10] J. Skilling and S. F. Gull, in *Maximum-Entropy and Bayesian Methods in Inverse Problems*, edited by C. R. Smith and W. T. Gandy, Jr. (Reidel, 1985).
[11] E. Artzy, T. Elfing, and G. T. Herman, Comp. Graph. Image Process. **11**, 242 (1979).
[12] M. F. Hutchinson, ACM Trans. Math. Software **12**, 150 (1986).

Downloaded 08 Nov 2012 to 194.81.223.66. Redistribution subject to AIP license or copyright; see http://rsi.aip.org/about/rights_and_permissions